

Optimization of conditions for *in vitro* modelling of subgingival normobiosis and dysbiosis

Divya Baraniya

Temple University

Thuy Do

University of Leeds

Tsute Chen

Forsyth Institute

Jasim Albandar

Temple University

Susan Chialastri

Temple University

Deirdre A. Devine

University of Leeds

Philip D. Marsh

University of Leeds

Nezar Al-hebshi (✉ alhebshi@temple.edu)

Temple University

Research Article

Keywords: Biofilm, Dysbiosis, High-Throughput Nucleotide Sequencing, Microbiota, Periodontitis

Posted Date: September 1st, 2022

DOI: <https://doi.org/10.21203/rs.3.rs-2011416/v1>

License:  This work is licensed under a Creative Commons Attribution 4.0 International License.

[Read Full License](#)

Abstract

Modeling subgingival microbiome in health and disease is key to identifying the drivers of dysbiosis and to studying microbiome modulation. Here, we optimize growth conditions of our previously described *in vitro* subgingival microbiome model.

Subgingival plaque samples from healthy and periodontitis subjects were used as inocula to grow normobiotic and dysbiotic microbiomes in MBEC assay plates. Saliva supplemented with 1%, 2%, 3.5% or 5% (v/v) heat-inactivated human serum was used as a growth medium under shaking or non-shaking conditions. The microbiomes were harvested at 4, 7, 10 or 13 days of growth (384 microbiomes in total) and analyzed by 16S rRNA gene sequencing.

Biomass significantly increased as a function of serum concentration and incubation period. Independent of growth conditions, the health- and periodontitis-derived microbiomes clustered separately with their respective inocula. Species richness/diversity slightly increased with time but was adversely affected by higher serum concentrations especially in the periodontitis-derived microbiomes. Microbial dysbiosis increased with time and serum concentration. *Porphyromonas* and *Alloprevotella* were substantially enriched in higher serum concentrations at the expense of *Streptococcus*, *Fusobacterium* and *Prevotella*. An increase in *Porphyromonas*, *Bacteroides* and *Mogibacterium* accompanied by a decrease in *Prevotella*, *Catonella* and *Gemella* were the most prominent changes over time. Shaking had only minor effects. Overall, the health-derived microbiomes grown for 4 days in 1% serum, and periodontitis-derived microbiomes grown for 7 days in 3.5%-5% serum were the most similar to the respective inocula.

In conclusion, normobiotic and dysbiotic subgingival microbiomes can be grown reproducibly in saliva supplemented with serum, but time and serum concentration need to be adjusted differently for the health and periodontitis-derived microbiomes to maximize similarity to *in vivo* inocula. The optimized model could be used to identify drivers of dysbiosis, and to evaluate interventions such as microbiome modulators.

Introduction

The oral microbiome is complex and diverse, but remains balanced over time (normobiosis), generally existing in a harmonious and mutually beneficial relationship with the host. However, this mutualistic relationship can breakdown due to changes in the balance of the microbiome and/or to the integrity of the host defenses (dysbiosis), and this increases the risk of disease [1]. The wide scale application of next generation sequencing technologies has revolutionized our understanding of the composition of the oral microbiome in health and disease. In periodontitis, dysbiosis is associated with increases in predominantly anaerobic, Gram-negative bacteria including *Treponema* spp., *Fretibacterium* spp., *Porphyromonas gingivalis*, *Tannerella forsythia* and *Desulfobulbus* spp. at the expense of facultative Gram-positive species belonging to the genera *Actinomyces* and *Streptococcus* [2, 3].

However, the drivers of subgingival microbial dysbiosis, which could make novel targets for interventions, are still not well understood. Likewise, the potential for microbiome modulators, such as prebiotics and probiotics, to reverse dysbiosis or maintain normobiosis as a treatment and/or prevention strategy for periodontitis has been minimally explored. Addressing these gaps in clinical studies is challenging due to the wide range of variables that can affect the oral microbiome. Potential interventions need to be tested in a preclinical environment, and therefore, validated *in vitro* microbiome models are important research tools in this respect. Various attempts have been made to model oral microbial communities including continuous flow models, static models or more recent sophisticated models that are based on microfluidics or impedance-based technologies [4]. Over the last 20 years, some static biofilm models (e.g., microtiter plates or the Calgary Biofilm Device) have become popular due to their ease of performance and high throughput [4]. Combined with the use of saliva or oral biofilms as inocula, these static models have been used successfully to generate highly diverse *in vitro* microbiomes that approximate to the complexity and community structure of clinical samples [5–10].

We recently developed an *in vitro* model of the subgingival microbiome in which health- and periodontitis-derived microbiomes are grown in parallel in a high throughput format [9], which can be used to study the dynamics and drivers of subgingival dysbiosis and, more importantly, to screen for microbiome modulators especially when combined with our recently described subgingival microbial dysbiosis index [3]. In the latter model, we found that saliva supplemented with 5%-20% (v/v) heat-inactivated human serum outperformed nutrient rich media, including BHI (Brain Heart Infusion) and SHI, in terms of maintaining viability of the biofilms, maximizing species diversity, and replicating normobiosis and dysbiosis. Nevertheless, it was observed that these relatively high serum concentrations led to the enrichment of *P. gingivalis* in a dose-dependent manner which tended to increase dysbiosis scores specially in the health-derived microbiomes.

In this study, we further explored the nutritional drivers of subgingival dysbiosis by lowering serum concentration, varying the incubation periods and evaluating the impact of shaking, with the aim of maximizing similarity to *in vivo* microbiomes. By running two biological replicates, we also aimed to demonstrate the reproducibility and utility of the model in generating subgingival normobiotic and dysbiotic microbiomes.

Methods

Study design and ethics statement

Figure 1 provides an overview of study design and workflow. Subgingival dental plaque samples were collected from patients that were being treated at the Dental Clinics of the Kornberg School of Dentistry, Department of Periodontics, Temple University, Philadelphia, USA, after obtaining informed consents. The study was approved by Temple University's Institutional Review Board under protocol #25586.

Sterile pooled human saliva (SPHS)

Unstimulated saliva was collected in sterile containers from ten dentally healthy volunteers, who had no severe cavities, no more than slight, localized gingivitis, no pocket depth or attachment loss ≥ 3 mm and no history of periodontitis. Additionally, participants were asked to not consume food, juice or caffeinated drinks within two hours prior to donating saliva samples. The samples were placed on ice immediately after collection, and transferred to the laboratory where they were pooled, treated with dithiothreitol at 2.5mM, filter sterilized, and stored at -20°C until used in the study.

Clinical inocula

For each experiment, subgingival plaque samples were collected from five subjects with moderate to severe periodontitis (defined as having at least one tooth per quadrant with bleeding on probing, pocket depth ≥ 5 mm and attachment loss ≥ 4 mm) and from 5 periodontally healthy subjects (defined as having no more than slight gingivitis, no probing pocket depth or attachment loss ≥ 3 mm and no previous history of periodontitis). The samples were collected using paper points and placed in 1 ml of reduced transport fluid (RTF) as previously described [9]. The two sets of samples, one from healthy subjects and the other from periodontitis individuals, were pooled separately and mixed by vortexing, yielding two homogenous suspensions which were used as a final inoculum for health- and periodontitis-derived biofilms, respectively. Samples were obtained from a completely different set of subjects for the two experiments (biological replicates).

Culture media

Heat inactivated human serum (Sigma, USA) was added to SPHS prepared as described above at final concentrations of 1%, 2%, 3.5% and 5% (v/v) to obtain a total of four different growth media.

Growth of *in vitro* microbiomes

Health- and periodontitis-derived microbiomes were grown on hydroxyapatite-coated pegs of MBEC plates (Innovotech, Edmonton, Canada) as described before [9]. Briefly, the pegs were preconditioned by immersing in SPHS for 16 hours before they were transferred to a 96 well plate containing 170 μl culture medium plus 10 μl inoculum per well in triplicates according to the layout shown in **Fig. 1**; the outer wells were filled with sterile PBS to prevent evaporation. No-inoculum control wells were spiked with 10 μl sterile RTF. The microbiomes were grown anaerobically for 4, 7, 10 or 13 days (four different plates) under shaking or non-shaking conditions (two sets of plates). The pegs with microbiomes were harvested at the end of each time point, washed with PBS for 15 seconds and immediately stored at -80°C for further analysis. The experiment was performed twice with two different sets of clinical inocula (biological replicates), yielding a total of 384 *in vitro* microbiomes.

DNA extraction and biomass assessment

Pegs with the grown microbiomes were each snapped off from the lid, placed in 1.5 ml tubes containing 180 μl lysozyme solution (20 mg/ml; Sigma, USA) and incubated for 30 minutes at 37°C . DNA was extracted from the lysate using Purelink Genomic DNA mini Kit (Invitrogen, Waltham, USA) according to

the manufacturer's instructions. DNA was quantified using Qubit 2.0 Fluorimeter and stored at -80°C until subjected to further analysis. Biomass was measured in terms of DNA yield (ng/microbiome).

Sequencing and data analysis

Degenerate primers 27FYM [11] and 519R [12] with index sequences were used for amplifying the V1-V3 region of the 16S rRNA gene, and the resultant indexed amplicon libraries were sequenced on an Illumina Miseq platform using 2*300 bp chemistry at the Integrated Microbiome Resource (IMR, Halifax, Canada). Resultant paired-end reads were merged with PEAR [13] and pre-processed (trimming, quality filtration, and chimera check) with mothur [14] as previously described [15]. The high-quality reads were then classified to the species level using our previously described BLASTn-based algorithm [15, 16]. Taxonomy tables and alpha diversity analysis were generated using Quantitative Insights into Microbial Ecology (QIIME2) [17]. The Subgingival Microbial Dysbiosis Index (SMDI) was calculated for the individual samples as previously described [3]. For assessing beta diversity, principal component analysis (PCA) was performed on centered log-ratio (CLR) species counts using microbiome [18] and phyloseq [19] packages in R. MaAsLin2 [20] was applied to CLR-transformed data to identify independent associations with each of the study variables (serum concentration, time points and shaking).

Results

Sequencing and data preprocessing statistics

A total of 26,208,640 paired-end reads were obtained (31,804 to 1,23,233 reads/sample), of which 95.24% reads merged successfully. Around 17% (4,310,661) of the sequences passed our stringent quality filtration, resulting in a final sequencing depth of 4,681 to 20,450 reads/sample. Raw sequences were submitted to Sequence Read Archive (SRA) under submission no. SUB11981103 (in process).

General microbial profiles of the inocula and *in vitro* microbiomes

A total of 119 and 137 species belonging to 39 and 40 genera and 8 phyla were detected in the two health inocula, respectively; in the two periodontitis inocula, 178 and 172 species, 55 and 65 genera, and 9 phyla were identified, respectively. In the *in vitro*-grown microbiomes, the comparable profiles were 58–103 species, 20–33 genera, 4–7 phyla in the health-derived microbiomes, and 75–135 species, 32–52 genera and 6–8 phyla in the periodontitis-derived microbiomes. The relative abundances and detection frequencies of identified phyla, genera and species in each of the samples are listed in **Supplementary Files 1–3**, respectively, while the average taxonomic profiles in the inocula as well as *in vitro* microbiomes as a function of serum concentration, incubation period and shaking are presented in **Supplementary Figs. 1 and 2**, for the phylum- and genus-level, respectively.

Firmicutes, Fusobacterium, and Bacteroidetes, in this order of abundance, were the most dominant phyla in health in both the clinical inocula as well as *in vitro* microbiomes. The same phyla were also the most abundant in periodontitis but in the order of Bacteroidetes, Firmicutes and Fusobacterium by abundance. However, in both health and periodontitis, these three phyla were over-represented in the *in vitro*

microbiomes at the expense of the Saccharibacteria, Proteobacteria and Actinobacteria (**Supplementary Fig. 3**). Chloroflexi was exclusively detected in the periodontitis inoculum but not in the respective *in vitro* microbiomes. At the genus level, *Fusobacterium*, *Streptococcus*, *Porphyromonas*, *Prevotella*, and *Alloprevotella* were the most abundant overall, although their relative abundances differed between health and disease and between the clinical inocula and the *in vitro* microbiomes (**Supplementary Figs. 2**). The latter showed enrichment of *Fusobacterium* and *Prevotella* in addition to *Mogibacterium*, *Catonella* and *Bacteroides* at the expense of *Leptotrichia*, *Rothia*, *Haemophilus*, *Capnocytophaga* and TM7 genera 1 and 5 (**Supplementary Fig. 3**).

At the species level, the dominant species in the health-derived microbiomes on average were *Fusobacterium periodonticum*, *Fusobacterium nucleatum*, *Streptococcus dentisani*, *Mogibacterium diversum*, *Porphyromonas endodontalis*, *Alloprevotella tanneriae*, *Porphyromonas* oral taxon 278, *Prevotella intermedia*, *Streptococcus* oral taxon 058, *Catonella morbi*, and *Veillonella parvula_group*, while periodontitis derived microbiomes were dominated by *Prevotella intermedia*, *Porphyromonas gingivalis*, *Bacteroides heparinolyticus*, *Bacteroides zooglyphiformans*, *Fusobacterium nucleatum*, *Fusobacterium periodonticum*, *Streptococcus tigurinus*, and *Peptoniphilaceae* oral taxon 790.

In vitro microbiomes replicate subgingival normobiosis and dysbiosis

Regardless of growth conditions, the health- and periodontitis-derived microbiomes along with the respective clinical inocula formed two separate main clusters in beta diversity analysis, accounting for ~32% variation along principal component 1 (Fig. 2A) – the biological replicates formed sub-clusters within each cluster and accounted for less variation (14% along principal component 2), primarily in periodontitis. Similarly, the health- and periodontitis-derived microbiomes reflected the differences between the respective inocula in terms of biomass, species richness (Chao index), alpha diversity (Shannon index) and dysbiosis (SMDI) (Fig. 2B), with all being significantly higher (with the exception of Shannon index) in the periodontitis-derived microbiomes.

More importantly, differential abundance analysis by MaAsLin2 identified microbial differences between the health- and periodontitis-derived *in vitro* microbiomes that are largely consistent with known differences between periodontitis and health *in vivo* (Fig. 2C). For example, *P. gingivalis*, *P. intermedia*, *Treponema denticola*, *Filifactor alocis*, *Fretibacterium fastidiosum*, *Pyramidobacter piscolens*, and *Mogibacterium timidum*, which have been consistently implicated as pathogens in periodontitis, were all significantly enriched in the periodontitis-derived microbiomes. Likewise, species such as *Porphyromonas catoniae*, *Streptococcus dentisani*, *S. sanguinis*, *Streptococcus* oral taxon 58, *Catonella morbi* and *Granulicatella adiacens*, which are typically health-associated species, were significantly enriched in the health-derived microbiomes. Figure 3 presents the relative abundances of selected differentially abundant genera and species. The latter were chosen to represent sister species (i.e. two species within the same genus) that showed opposite enrichment in the health- and periodontitis-derived microbiomes consistent with differences demonstrated in their preponderance *in vivo*.

Higher serum concentration and longer incubation time promote dysbiosis

Generalized linear modelling or MaAslin2, as appropriate, were used to identify the independent effects of serum and incubation time on the different microbial parameters assessed, applying a false discovery rate (FDR) cutoff of 0.1 when applicable. Biofilm biomass significantly increased with time and with increasing serum concentrations for both the health- and periodontitis-derived microbiomes (Fig. 4A). Species richness (Chao index) did not change by time and serum concentration in the health-derived microbiomes, but it significantly dropped in 5% serum and after days 10 and 13 incubation in the periodontitis-derived microbiomes (Fig. 4B). Alpha diversity (Shannon index) significantly decreased in days 7 and 10, increased at 2% and 3.5% serum but dropped at 5% in the health-derived microbiomes; however, the magnitude of changes was small (Fig. 4C). In the periodontitis-derived microbiome, the Shannon index substantially increased with time but markedly decreased as a function of serum concentration. Dysbiosis (SMDI) increased proportionally as a function of time and serum concentration, in both the health-derived and periodontitis-derived microbiomes grown *in vitro* (Fig. 4D), being closest to the respective clinical inocula in the health-derived-microbiomes when grown in 1% serum for 4 days (Median SMDI of -1 in the *in vitro* microbiomes compared to -2.2 in the health inoculum), and in the periodontitis-derived-microbiomes after growth in 1% serum for 13 days (Median SMDI of 1.33 in the microbiomes compared to 1.38 in the periodontitis inoculum); those grown in 3.5%-5% for 7 days or 2% for 10 days came next (SMDI ~ 1.25). Beta diversity analysis for health and periodontitis separately resulted in two main clusters by biological replicate along PC1 and sub-clusters by growth time along PC2 (Fig. 4E); analysis of the distance-matrix revealed that the health-derived microbiomes grown for 4 days at 1% serum concentration and the periodontitis-derived microbiomes grown for 4 days in 5% serum (followed by those grown in 5% for 7 days or 2% for 10 days) were the closest to the respective clinical inocula.

The relative abundances of phyla and genera that significantly changed as a function of time and serum concentration are shown in **Supplementary Fig. 4** and **Fig. 5**, respectively. At the phylum level, serum resulted in a dose-dependent increase in Bacteroidetes at the expense of Firmicutes and Fusobacteria, while a prolonged growth period was associated with an increase of Actinomyces and Spirochetes and slight decrease in Firmicutes, Fusobacteria and Bacteroidetes. At the genus-level, the major changes included substantial enrichment of *Porphyromonas* and *Alloprevotella* as a function of serum concentration at the expense of *Streptococcus*, *Fusobacterium* and *Prevotella*, and an increase in *Porphyromonas*, *Bacteriodes* and *Mogibacterium* accompanied by a decrease in *Prevotella*, *Catonella* and *Gemella* as a function of time. Figure 6 presents selected sister species that responded in opposite directions to increased serum concentration and incubation period.

Shaking had limited effect on composition of the *in vitro* microbiomes

The independent effects of shaking on the growing microbiomes is shown in **Supplementary Fig. 5**. Shaking increased biomass of the health-derived microbiome but not of the periodontitis-derived

microbiomes. Statistically significant differences were observed for species richness and dysbiosis, but the magnitude of change was minor. Namely, shaking slightly increased in Chao index in the health-derived microbiomes and slightly decreased it in the periodontitis-derived microbiomes, while it marginally increased SMDI in both the health- and periodontitis-derived microbiomes, probably because of enrichment of genera *Treponema* and *Pyramidobacter* at the expense of *Gemella* and *Granulicatella* (Supplementary Fig. 6). Shaking did not affect alpha diversity (Shannon index) in either microbiome type.

Discussion

Periodontal diseases are associated with an increase in subgingival biomass and a shift in the overall balance of the composition of the biofilm [2]. The factors that drive the development of this dysbiotic community could include changes in the status of the host defenses but probably also include changes to the nutritional profile in the local environment to enable the fastidious, disease-associated microbes to be able to grow and to outcompete the species associated with health. While the primary purpose of the present study was to optimize conditions for modeling the subgingival microbiome, it also enabled us to assess the potential role of nutrients as drivers of subgingival microbial dysbiosis.

Saliva is a major nutritional source for oral micro-organisms, but the healthy gingival crevice is also exposed to small quantities of a serum-like exudate via the flow of gingival crevicular fluid (GCF) [1]. During periodontal inflammation, the flow of GCF is increased markedly. Apart from delivering components of the host defenses, this exudate is important nutritionally and is capable of supporting the growth of proteolytic and fastidious bacteria. Early studies demonstrated that growing subgingival microbiota in the presence of serum enriched for *Bacteriodes*, *Peptostreptococcus* and *Fusobacterium* [21]. Along the same lines, recent studies by our group and others have shown that adding serum to a medium results in significant enrichment of periodontal pathogens, including *P. gingivalis* [9, 22, 23]. In our previous study [9], it was established that saliva with serum outperformed other nutrient-rich media for modeling subgingival biofilms, both from health and disease; nonetheless, serum, even at the lowest concentration (5%) still resulted in overgrowth of *P. gingivalis*, especially in the health-derived microbiomes.

Consequently, in this study we used lower concentrations of serum in saliva, and also varied the length of incubation and evaluated the impact of shaking during biofilm development. Composition of the *in vitro* microbiomes were quantified in far greater detail and at a finer resolution than our previous study. The major findings of the study are as follows. First, the study demonstrates the reliability of the model to reproducibly generate normobiotic and dysbiotic subgingival microbiomes *in vitro*. Second, the health-derived and periodontitis-derived microbiomes have different requirements for maintaining their community structure. Overall, and taking into consideration species richness, alpha and beta diversity and SMDI values, the health-derived microbiomes grown for 4 days at 1% serum were closest to the health inoculum, while for periodontitis, the microbiomes grown for 7 days at 35%-5% serum, or for 10 days at 1%-2% serum, were comparable and the most similar to the respective inoculum. The third important finding is that serum and time independently and differently contributed to dysbiosis. For

example, while *P. gingivalis* increased as a function of both factors, *Treponema*, *Fretibacterium*, and *Pyramidobacter* increased primarily as a function of time, while *Tannerella* and *Selenomonas* increased with serum concentration. There were taxa that changed in opposite directions. For examples, *Veillonella* increased with serum concentration but decreased with time.

Apart from dysbiosis, the temporal microbial changes observed in the *in vitro* microbiomes are consistent with those reported for *in vivo* biofilms. For instance, during the early stages of oral biofilm development, *Firmicutes* including *Streptococcus* and *Veillonella* are primary colonizers [24]. Other bacteria actively involved in early stages include *Actinomyces*, *Gemella*, *Granulicatella*, *Neisseria*, *Prevotella*, and *Rothia* [25]. In this study, these early colonizers were significantly higher in abundance on Day 4 than at later time points. *Fusobacterium* species are considered as “bridge organisms” between early and late colonizers, which facilitates the growth of late colonizers by creating a conducive environment using its ability to coaggregate with most other species [26, 27]. Here, *Fusobacterium* increased during early biofilm development, though this was followed by a decrease in abundance over time. Late colonizers include many periodontal pathogens such as *Porphyromonas*, *Tannerella*, and *Treponema* [27], which in our study were significantly more abundant on days 10 and 13 relative to days 4 and 7.

As expected, and although the model captured much of the species richness and diversity of the clinical inocula, there were a few species which did not thrive and, as discussed above, some species which were enriched in the *in vitro* biofilms, and this implies that there are other factors that determine the composition of the subgingival microbiome *in vivo*. This is a limitation of our (and of others) model [4], but the system described here also provides the opportunity to further explore these factors including components of the host defenses. Overall, the close similarity of the developing biofilms to the microbiomes reported *in vivo* in health and disease means that the model could be used to investigate potential interventions to prevent or reverse dysbiosis.

In conclusion, this study demonstrates that saliva supplemented with heat-inactivated serum can be used to reliably and reproducibly grow normobiotic and dysbiotic subgingival microbiomes from clinical samples. However, serum and incubation periods need to be adjusted differently for the health- and periodontitis-derived microbiomes to maximize their similarity to *in vivo* biofilms. The study also shows that time and serum are independent drivers of dysbiosis. This model is an easy and effective system to study subgingival biofilm colonization in disease and health, and to evaluate interventions to prevent or reverse dysbiosis.

Declarations

Data availability statement

Raw data generated from this study has been deposited to and is publically available from Sequence Read Archive (SRA) under submission no. SUB11981103 (in process).

Ethics statement

The study was approved by Temple University's Institutional Review Board under protocol 25586.

Authors' contributions

DB contributed to design, data acquisition, analysis and interpretation, and drafted the manuscript; TC contributed to data analysis, and critically revised the manuscript; JMA and SMC contributed to data acquisition, and critically revised the manuscript; TD, DAD and PDM contributed to design and data interpretation, and critically revised the manuscript; NNA, conceived the study and contributed to design, data analysis and interpretation, and critically revised the manuscript. All authors gave final approval and agree to be accountable for all aspects of the work.

Funding

This study was supported by the National Institute of Dental and Craniofacial Research (grant 1R03DE028379)

Conflict of interest

None to declare

References

1. Kilian, M., et al., *The oral microbiome - an update for oral healthcare professionals*. Br Dent J, 2016. **221**(10): p. 657–666.
2. Curtis, M.A., P.I. Diaz, and T.E. Van Dyke, *The role of the microbiota in periodontal disease*. Periodontol 2000, 2020. **83**(1): p. 14–25.
3. Chen, T., P.D. Marsh, and N.N. Al-Hebshi, *SMDI: An Index for Measuring Subgingival Microbial Dysbiosis*. J Dent Res, 2022. **101**(3): p. 331–338.
4. Brown, J.L., et al., *Polymicrobial oral biofilm models: simplifying the complex*. J Med Microbiol, 2019. **68**(11): p. 1573–1584.
5. Edlund, A., et al., *An in vitro biofilm model system maintaining a highly reproducible species and metabolic diversity approaching that of the human oral microbiome*. Microbiome, 2013. **1**(1): p. 25.
6. Tian, Y., et al., *Using DGGE profiling to develop a novel culture medium suitable for oral microbial communities*. Mol Oral Microbiol, 2010. **25**(5): p. 357–67.

7. Kistler, J.O., M. Pesaro, and W.G. Wade, *Development and pyrosequencing analysis of an in-vitro oral biofilm model*. BMC Microbiol, 2015. **15**: p. 24.
8. Kolderman, E., et al., *L-arginine destabilizes oral multi-species biofilm communities developed in human saliva*. PLoS One, 2015. **10**(5): p. e0121835.
9. Baraniya, D., et al., *Modeling Normal and Dysbiotic Subgingival Microbiomes: Effect of Nutrients*. J Dent Res, 2020. **99**(6): p. 695–702.
10. Walker, C. and M.J. Sedlacek, *An in vitro biofilm model of subgingival plaque*. Oral Microbiol Immunol, 2007. **22**(3): p. 152–61.
11. Frank, J.A., et al., *Critical evaluation of two primers commonly used for amplification of bacterial 16S rRNA genes*. Appl Environ Microbiol, 2008. **74**(8): p. 2461–70.
12. Lane, D.J., et al., *Rapid determination of 16S ribosomal RNA sequences for phylogenetic analyses*. Proc Natl Acad Sci U S A, 1985. **82**(20): p. 6955–9.
13. Zhang, J., et al., *PEAR: a fast and accurate Illumina Paired-End reAd mergeR*. Bioinformatics, 2014. **30**(5): p. 614–20.
14. Schloss, P.D., et al., *Introducing mothur: open-source, platform-independent, community-supported software for describing and comparing microbial communities*. Appl Environ Microbiol, 2009. **75**(23): p. 7537–41.
15. Al-Hebshi, N.N., et al., *Inflammatory bacteriome featuring Fusobacterium nucleatum and Pseudomonas aeruginosa identified in association with oral squamous cell carcinoma*. Sci Rep, 2017. **7**(1): p. 1834.
16. Al-Hebshi, N.N., et al., *Robust species taxonomy assignment algorithm for 16S rRNA NGS reads: application to oral carcinoma samples*. J Oral Microbiol, 2015. **7**: p. 28934.
17. Caporaso, J.G., et al., *QIIME allows analysis of high-throughput community sequencing data*. Nat Methods, 2010. **7**(5): p. 335–6.
18. Leo Lahti, S.S., *Tools for microbiome analysis in R*. 2017: <https://github.com/microbiome/microbiome/>.
19. McMurdie, P. and S. Holmes, *Phyloseq: An R Package for Reproducible Interactive Analysis and Graphics of Microbiome Census Data*. PloS one, 2013. **8**: p. e61217.
20. Mallick, H., et al., *Multivariable association discovery in population-scale meta-omics studies*. PLoS Comput Biol, 2021. **17**(11): p. e1009442.
21. ter Steeg, P.F., et al., *Enrichment of subgingival microflora on human serum leading to accumulation of Bacteroides species, Peptostreptococci and Fusobacteria*. Antonie Van Leeuwenhoek, 1987. **53**(4): p. 261–72.
22. Naginyte, M., et al., *Enrichment of periodontal pathogens from the biofilms of healthy adults*. Sci Rep, 2019. **9**(1): p. 5491.
23. Cieplik, F., et al., *Microcosm biofilms cultured from different oral niches in periodontitis patients*. J Oral Microbiol, 2019. **11**(1): p. 1551596.

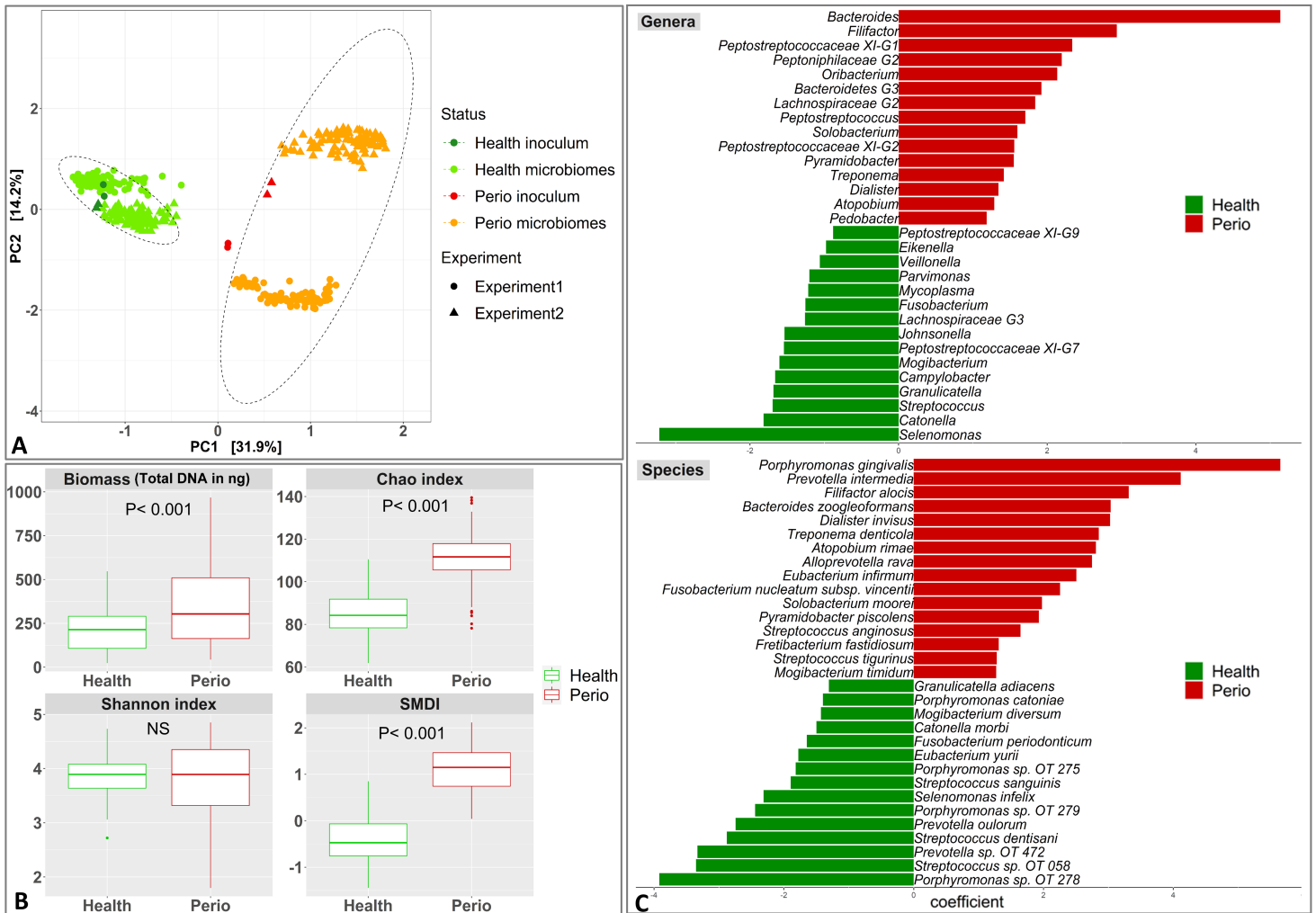


Figure 2

In vitro microbiomes from health and periodontitis. **A** Principal component analysis (PCA) plots based on centered log-ratio (CLR) transformed data as a function of health status and experimental replicates. **B** Boxplots of biomass, alpha diversity indices, and subgingival microbial dysbiosis index (SMDI) in the health- and periodontitis-derived microbiomes. Statistical comparisons were performed using Mann-Whitney test. **C** Top differentially abundant genera and species between the health- and periodontitis-derived microbiomes with FDR value < 0.1 and coefficient > 2 or < -2 (MaAsLin2 analysis on CLR transformed data with health status, biological replicate, medium, shaking and incubation time as fixed effects and technical replicates as random effects). Plots were produced with R.

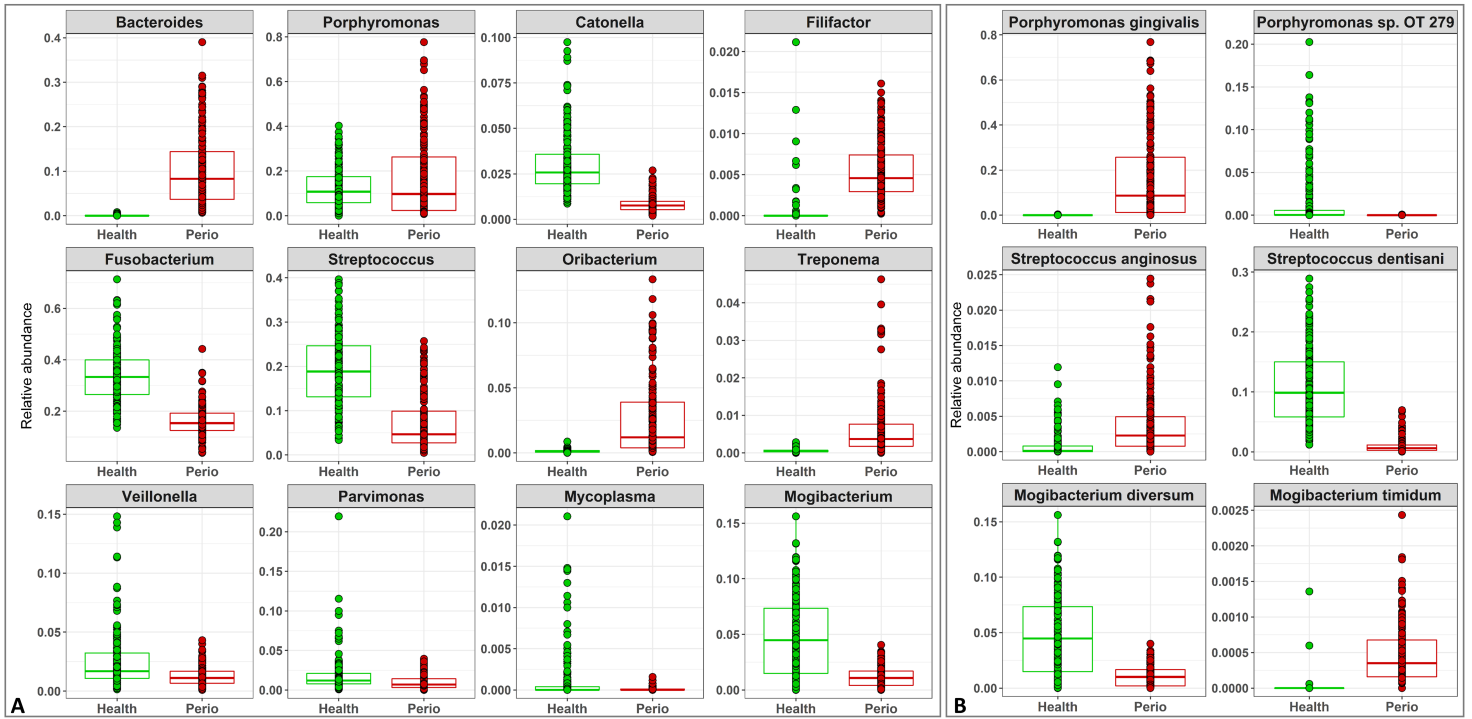


Figure 3

Selected differentially abundant taxa in the periodontitis and health-derived microbiomes. Centered log-ratio (CLR) transformed data were analyzed with MaAsLin2 including health status, biological replicate, medium, shaking, and incubation time as fixed effects and technical replicates as random effects. Relative abundances are shown for (A) 12 genera and (B) 3 pairs of ‘sister’ species that significant different (FDR value < 0.1) between the two groups. Plots were produced with R.

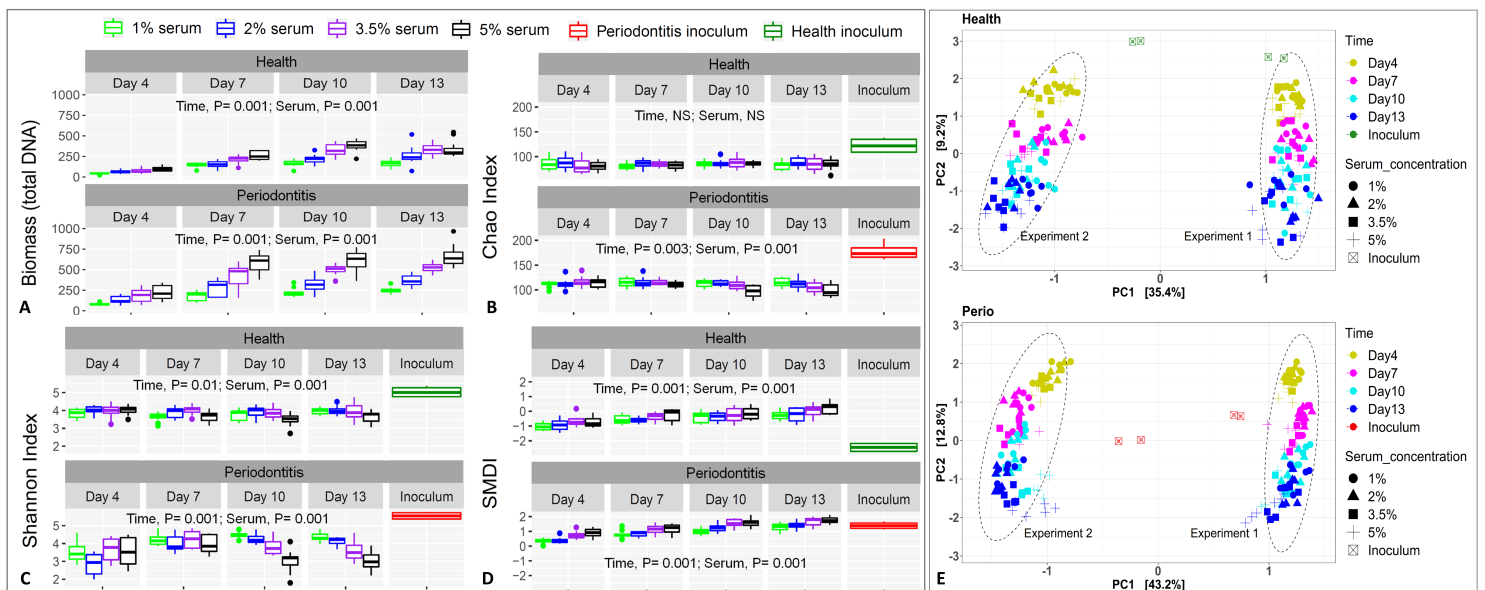


Figure 4

***In vitro* microbiome diversity as a function of serum concentration and incubation period.** Biomass (A), Chao Index (B), Shannon Index (C) and subgingival microbial dysbiosis index (SMDI, D) are presented as boxplots by serum concentration and time point for the health- and periodontitis-derived microbiomes separately. Statistical comparisons were performed using generalized linear models (multinomial distribution) with biological replicate, medium, shaking and time as covariates. E Principal component analysis (PCA) plots based on centered log-ratio (CLR) transformed data by serum concentration, time point and experimental replicate. Plots were produced with R.

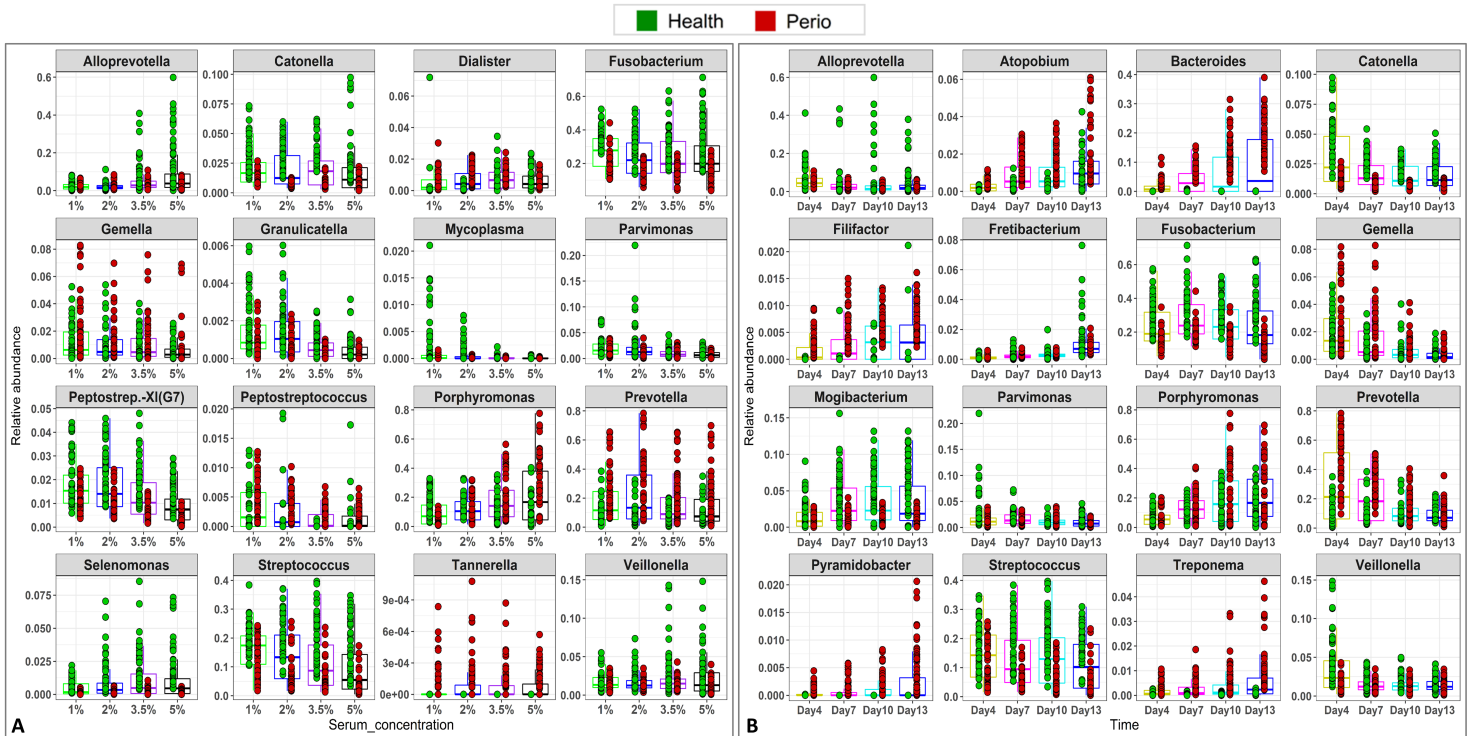


Figure 5

Selected differentially abundant genera by serum concentration and incubation period. Centered log-ratio (CLR) transformed data were analyzed with MaAsLin2 including health status, biological replicate, medium, shaking, and incubation time as fixed effects and technical replicates as random effects. Relative abundances are shown for 16 genera that significantly differed (FDR value < 0.1) by serum concentration (A) and 16 genera that differed by incubation period (B). Plots were produced with R.

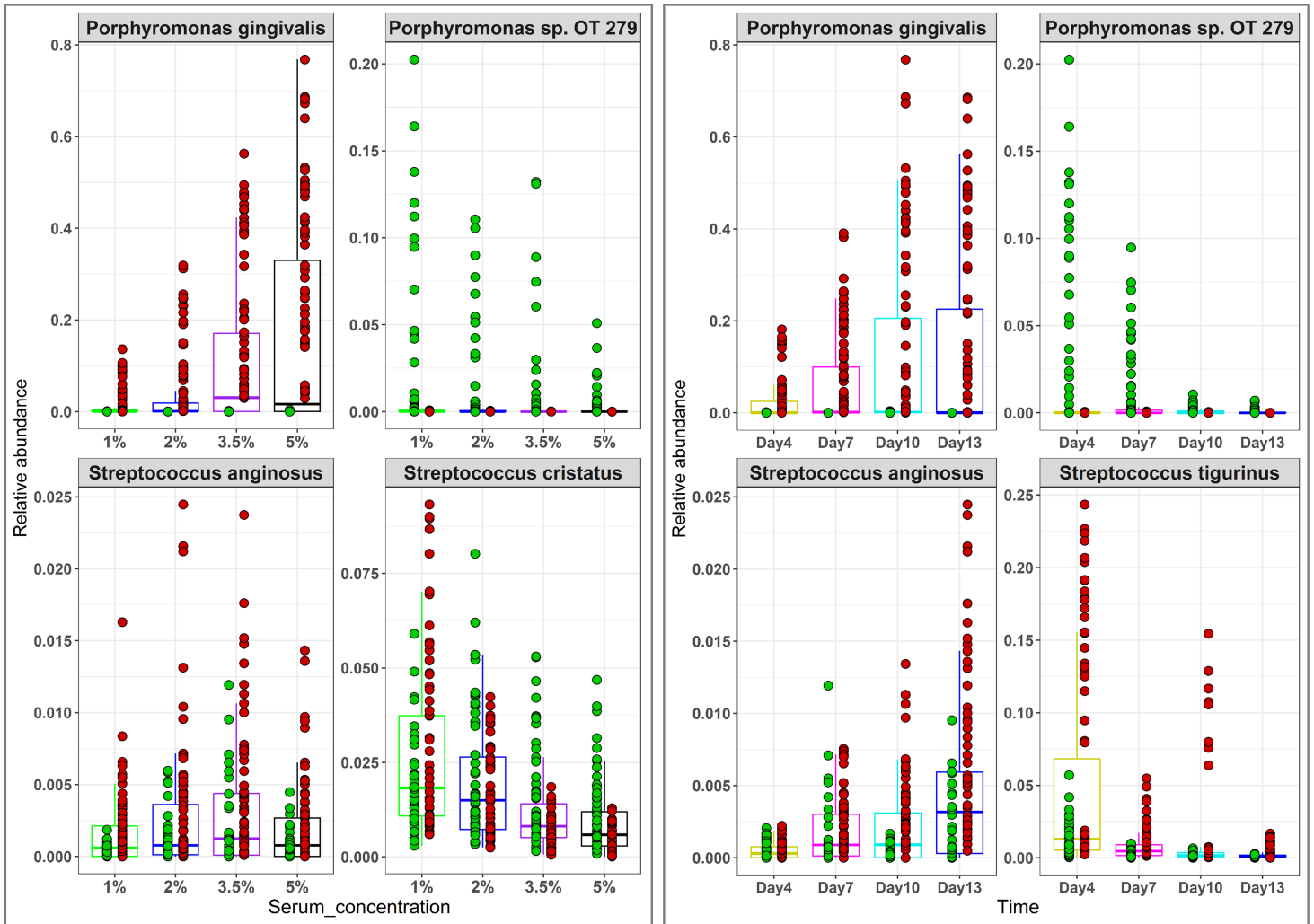


Figure 6

Selected differentially abundant species by serum concentration and incubation period. Centered log-ratio (CLR) transformed data were analyzed with MaAsLin2 including health status, biological replicate, medium, shaking, and incubation time as fixed effects and technical replicates as random effects. Relative abundances are shown for 4 pairs of ‘sister’ species that significant different (FDR value < 0.1) between the two groups. Plots were produced with R.

Supplementary Files

This is a list of supplementary files associated with this preprint. Click to download.

- [Supplementaryfigures.pptx](#)